

## Distributed Acoustic Sensing Signal Model Under Static Fiber Conditions

*A.ROBERT SAM**G.PUNITHAVATHY\***G.S.AYYAPPAN*

CSIR-CSIO Chennai

E-mail: punitha.105@gmail.com

**Abstract:** This paper presents a statistical model for distributed acoustic sensor interrogation units that utilizes laser pulses transmitted into fiber optics. Interactions within the fiber lead to localized acoustic energy, resulting in backscatter, which is a reflection of the light. Explicit equations were used to calculate the amplitudes and phases of backscattered signals. The proposed model accurately predicts the amplitude signal spectrum and autocorrelation, aligning well with experimental observations. This study also explores the phase signal characteristics relevant to optical time-domain reflectometry (OTDR) system sensing applications, demonstrating consistency with the experimental results. The experiments were conducted using Python coding, enabling the analysis of the individual components of the Distributed Acoustic Sensing (DAS) system.

The assumptions of the model include the static condition of the fiber, implying the absence of external forces or vibrations. Consequently, no external acoustic disturbances were considered. The backscattered signal comprises a random noise component resulting from intrinsic fiber imperfections, and a coherent component arising from the interplay between the laser pulse and the fiber.

Keywords: distributed acoustic sensing, fiber optics, optical time-domain reflectometry, Rayleigh scattering.

### Introduction

Distributed Acoustic Sensing (DAS) is a technology that employs fiber-optic cables to identify and localize acoustic signals across an entire cable length. The basic principle of a DAS involves transmitting a laser pulse to a fiber-optic cable and interacting with it to generate backscattered signals. These signals contain information regarding the acoustic energy absorbed by the fiber, and can be used to detect and locate acoustic events [1], such as vibrations or sound waves.

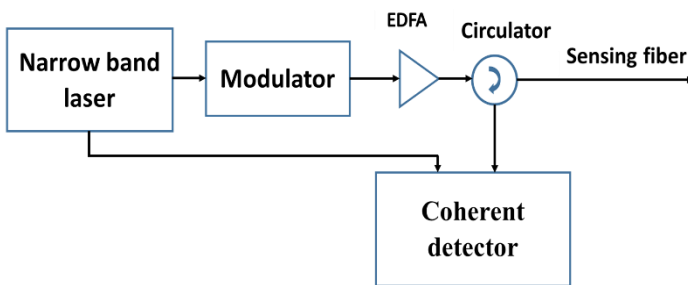
The DAS signal model under static fiber conditions describes the characteristics of backscattered signals generated in a fiber-optic cable when no acoustic disturbances are present. This model assumes that the fiber is in a static condition, that is, no external force or vibration is applied to the cable. Under these conditions, the backscattered signal consists of a random noise component [2] caused by the intrinsic imperfections of the fiber and a coherent component resulting from the laser pulse interacting with the fiber. The coherent component of the signal can be further divided into amplitude and phase components, which can be mathematically modeled using explicit equations [4]. The amplitude component represents the signal strength, and the phase component represents the signal timing. By analyzing these components, predictions can be made regarding the signal spectrum and autocorrelation characteristics. Overall, the DAS signal model under static fiber conditions provides a foundation for understanding the behavior of fiber-optic cables and their interaction with laser pulses [3], which is essential for developing and optimizing the DAS technology.

The term 'dynamic' refers to elements that can change or be altered during the program's execution, while 'static' refers to something that is fixed or unchanging during the program's execution [5]. In this study, we focused on a static model.

In this study, we discuss the following points:

1. Coherent narrow band laser source
2. Acousto-Optic modulator (AOM)
3. Erbium-Doped Fiber Amplifier (EDFA)
4. Propagation of light in single-mode fiber
5. Phase-based optical time domain reflectometry system

**Circuit diagram**



**Circuit diagram of entire DAS technology**

Figure 1 provides a concise and clear overview of the DAS architecture, helping us to understand how different components interact and contribute to the circuit. This circuit was used to simulate each stage of the signal model for analysis.

**1. Coherent narrowband laser sources**

To simulate a coherent source with a wavelength of 1550 nm [6], we must use the equation for an optical wave because it is an electromagnetic wave. The coherent source equation for an optical wave is generally expressed as a complex phasor representation of the electric field. Here's the equation:

$$E(t) = E_o \cdot \cos(2\pi ft + \phi) \text{ ----- (1.1)}$$

In the given expression, where  $E(t)$  represents the electric field amplitude at time  $t$ ,  $E_o$  is the peak electric field amplitude associated with the optical power of the laser,  $f$  denotes the optical frequency in Hertz,  $t$  is the time variable measured in seconds,  $\phi$  represents the phase angle of the optical wave in radians.

The optical power  $P$  of the laser in watts is related to the electric field  $E_o$  using the following equation:

$$P = \frac{1}{2} \epsilon_o cnA |E_o|^2 \text{ ----- (1.2)}$$

In the provided context, where  $\epsilon_o$ - (approximately  $8.854 \times 10^{-12}$  F/m),  $c$  - (approximately  $3 \times 10^8$  m/s),  $n$  is the refractive index of the laser medium (assumed to be constant at the center wavelength).

We calculate the electric field amplitude  $E_o$  by assuming a constant refractive index at the center wavelength and arbitrary cross-sectional area [7]. Subsequently, we generated coherent optical waveforms for both the minimum and maximum power levels, and plotted those using Python's built-in plotting function.

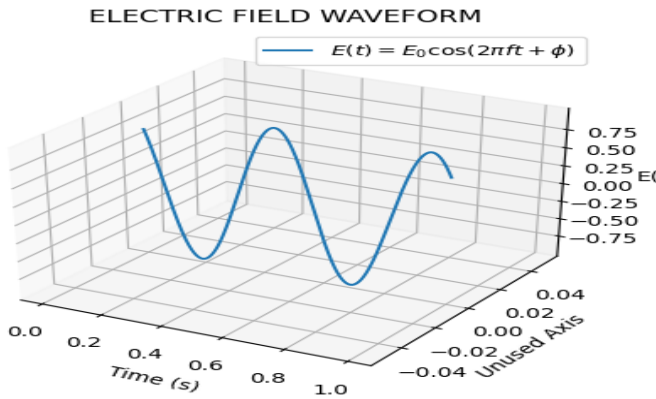


Figure 1.1 : Electric field waveform

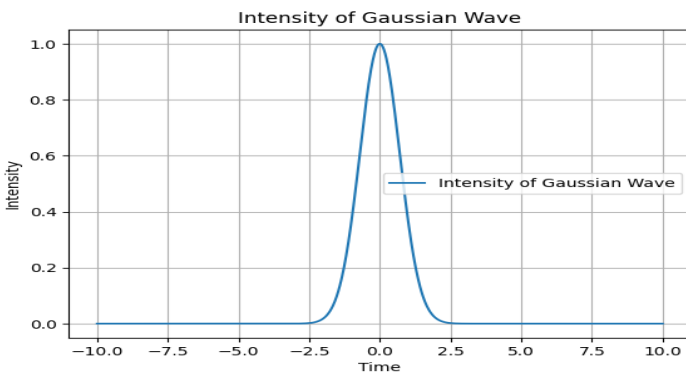


Figure 1.2: Gaussian waveform model

## 2. Acousto-Optic Modulator (AOM)

An Acousto-Optic Modulator (AOM) is a device that uses an acousto-optic effect to modulate optical signals. The refractive index of a material is modulated by the passage of an acoustic wave through the material. In AOM, an acoustic wave is generated and propagated through a material, typically a crystal, by applying a Radio Frequency (RF) signal to a piezoelectric transducer [8]. This acoustic wave interacts with the optical beam passing through the crystal, leading to changes in the properties of the beam, such as intensity, phase, or frequency. The AOM output waveform model depends on the specific type of designed modulation. Below are the two common modulation types and their respective equations.

In intensity modulation using an acousto-optic modulator (AOM), the application of a radio-frequency (RF) signal to the piezoelectric transducer initiates an acoustic wave within the crystal. This acoustic wave induces changes in the refractive index of the crystal, leading to alterations in the optical beam intensity as it propagates through the crystal. The modulation depth of intensity ( $\Delta I/I_0$ ) is quantified by the following equation:

$$\frac{\Delta I}{I_0} = m \cdot P_{RF} \quad \text{----- (2.1)}$$

Where:  $\Delta I / I_0$  = Relative intensity change (dimensionless)  $m$  = Modulation constant (change in intensity per unit RF power)  $P_{RF}$  = RF power applied to the AOM

Phase Modulation: In phase modulation using an AOM, the RF signal generates an acoustic wave that imparts a phase shift to the optical beam. The phase shift ( $\Delta\Phi$ ) was directly proportional to the RF frequency applied to the AOM and the distance covered by the acoustic wave within the crystal. The phase modulation can be described using the following equation:

$$\Delta\Phi = 2\pi \cdot f_{RF} \cdot d/v \quad \text{----- (2.2)}$$

where  $\Delta\Phi$  = Phase shift induced by the AOM (rad),  $f_{RF}$  is the RF frequency applied to the AOM (Hz),  $d$  is the distance traveled by the acoustic wave inside the crystal (m), and  $v$  is the acoustic velocity in the crystal (m/s).

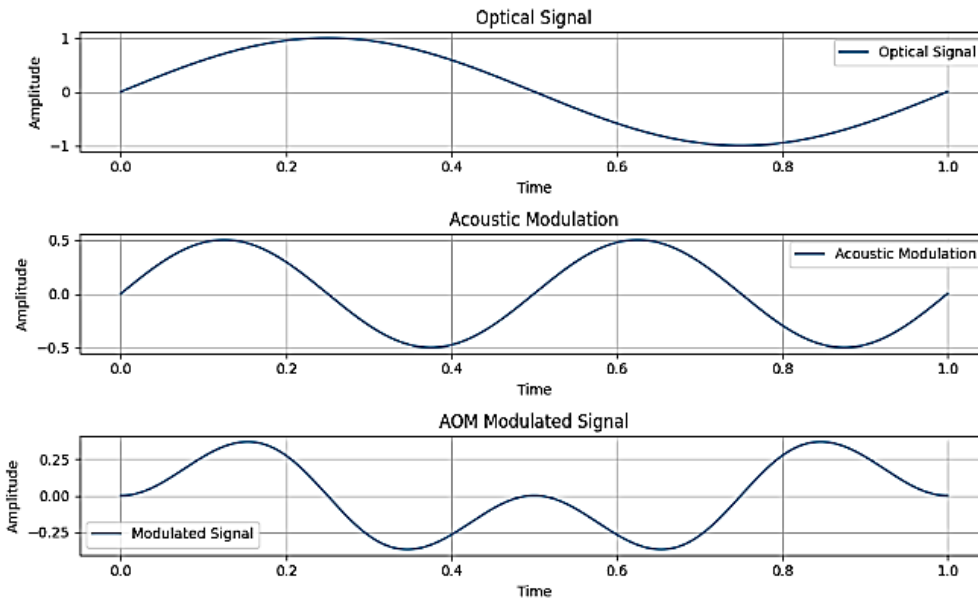


Figure 2.1: Acousto-Optic Modulator output signal diagram

### 3. Erbium-Doped Fiber Amplifier (EDFA):

An Erbium-Doped Fiber Amplifier (EDFA) is an optical fiber doped with Erbium ions. When pumped with an external light source, typically at wavelengths of 980 or 1550 nm, erbium ions become excited and amplify the optical signals passing through the doped fiber. Consequently, an EDFA can boost signal power without requiring electrical-to-optical conversion [9].

The amplification process in an EDFA is described by the following equation.

$$P_{out} = G * P_{in} \quad \text{----- (3.1)}$$

Where  $P_{out}$  is the output optical power after amplification and  $G$  is the gain of the EDFA, which represents the ratio of the output power to the input power.

The gain ( $G$ ) of an EDFA is generally expressed in decibels (dB) and can be calculated as:

$$G(dB) = 10 * \log_{10}(P_{out} / P_{in}) \quad \text{----- (3.2)}$$

EDFAs can achieve high gain levels, typically ranging from 20 to 30 dB or more. The gain is relatively constant over a wide range of input power levels, making EDFAs well suited for boosting optical signals in long-distance fiber-optic communication.

### 4. Propagation of light in single mode fiber

#### 4.1. Rayleigh scattering of light in a single-mode fiber

When light interacts with small particles or irregularities in a medium, it scatters in several manners. In single-mode optical fibers, Rayleigh scattering refers to the scattering of light caused by tiny fluctuations in the refractive index of the fiber core material. These fluctuations are typically caused by variations in the molecular density or impurities in the glass structure [10]. The intensity of the Rayleigh scattered light can be described by the Rayleigh scattering equation:

$$I(\theta) = I_0 * (\lambda / (4 * \pi * n * d))^2 * (1 + \cos^2\theta) \quad \text{----- (4.1)}$$

Rayleigh Scattering Loss (attenuation) Equation: The loss due to Rayleigh scattering in an optical fiber can be described by the following equation:

$$\alpha_R = \frac{8\pi^3}{3} \left(\frac{n_{core}}{\lambda}\right)^4 \left(\frac{n_{core}^2 - n_{clad}^2}{2n_{core}}\right)^2 \frac{\ln(1/v)}{A_{eff}} \quad \text{----- (4.2)}$$

where  $\alpha R$  is the Rayleigh scattering loss per unit length in decibels per meter (dB/m) and  $V$  is the normalized frequency (V-number) of the fiber, defined as  $V=2\pi a/\lambda \cdot n_{core}$ , where  $a$  is the radius of the fiber core and  $n_{core}$  is the refractive index of the core.  $A_{eff}$  is the effective mode area of the fiber mode in square meters [11]. This represents the area over which the guided mode is distributed within the fiber.

**4.2. The model for light scattering in a single-mode fiber under coherent radiation is introduced into the simulation as follows:**

**Coherent Source and Scattering:** When employing a coherent source, such as a laser, the scattering phenomenon within a single-mode fiber (SMF) can be conceptualized as the combined effect of scatterers randomly distributed along the length of the fiber. It is important to note that in this scenario, no spatial correlation exists between scatterers. This lack of spatial correlation contributes to the overall understanding of the cumulative scattering behavior within the SMF. In other words, each scatterer acts independently of the others [11].

**Impulse Response:** The impulse response of the system, denoted as  $h(t)$ , describes the response of the fiber to a short pulse of light. It is the sum of all scatterers (indexed by  $n$ ), and is represented by the following equation:

$$h(t) = \sum_{n=1}^N \alpha_{RS}(\tau_n) B(\tau_n) A(\tau_n) \exp[-V_g \tau_n \alpha_a] \delta(t - \tau_n) \quad \text{----- (4.3)}$$

**Simplification:** The first three terms of the impulse response (Equation 4.3) can often be combined into a single term, represented as:

$$h(t) = \sum_{n=1}^N a(\tau_n) \exp[-V_g \tau_n \alpha_a] \delta(t - \tau_n) \quad \text{----- (4.4)}$$

**Stochastic Model and Speckle:** The simplified equation (Equation 4.4) describes a stochastic model, similar to the phenomena of speckle. In this model, scatterers are considered complex Gaussian random variables with circular symmetry (CCRV), which exhibit circular symmetry and follow a Gaussian distribution in a random fashion, a simplification that streamlines the analysis.

**Spatial Distribution:** The scatterer positions in the fiber are assumed to follow a random uniform distribution, meaning that they are randomly distributed along the length of the fiber.

**Power Spectral Density:** The random uniform distribution of scatterers within the single-mode fiber facilitates the application of a relevant theorem for calculating the power spectral density of the light diffusion received from the random mode, as described in Equation 4.4.

This paper describes a light-scattering model in an SMF illuminated by a coherent source. It considers scatterers that are randomly distributed in the fiber, with each contributing independently to the impulse response. The model is stochastic in nature, similar to speckle phenomena, and enables the calculation of the power spectral density based on the random distribution of scatterers.

**5. Phase based optical time domain reflectometry system**

Phase-optical time-domain reflectometry encompasses the evaluation of both the intensity and phase of backscattered light, and is characterized in relation to both the time and distance within an optical fiber.

**Phase of the Backscattered Signal:** The phase of the backscattered signal at a given time ( $t$ ) and distance ( $z$ ) from the OTDR launch point is given by

$$phase(t, z) = 2\pi \cdot n \cdot \frac{t}{c} + 2\pi \cdot \Delta n \cdot \frac{t-z}{c} \quad \text{----- (5.1)}$$

where  $n$  is (assumed constant).  $c$  (approximately  $3 \times 10^8$  m/s).  $\Delta n$  is the refractive index perturbation (change in refractive index) at distance  $z$  from the launch point of the OTDR.

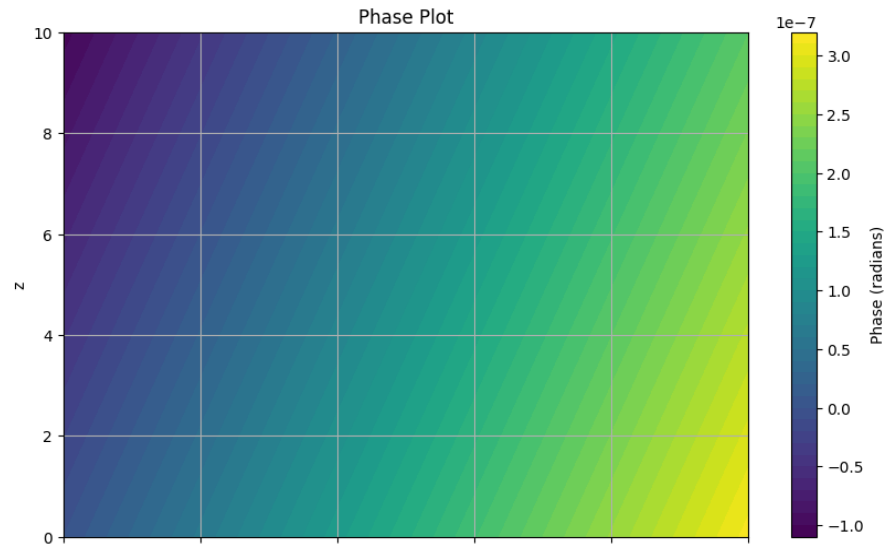


Figure 5.1 : Phase of the Backscattered signal

**Intensity of the Backscattered Signal:** The intensity of the backscattered signal at a given time (t) and distance (z) from the OTDR launch point is proportional to the square of the magnitude of the backscattered electric field [12]. It is given by:

$$intensity(t, z) = |E(t, z)|^2 \quad \text{----- (5.2)}$$

where  $E(t, z)$  is the electric field of the backscattered signal at time t and distance z from the launch point of OTDR. The electric field  $E(t, z)$  can be calculated as the sum of all the backscattered waves at different points along the fiber, each with different amplitudes and phases, depending on the refractive index variations.

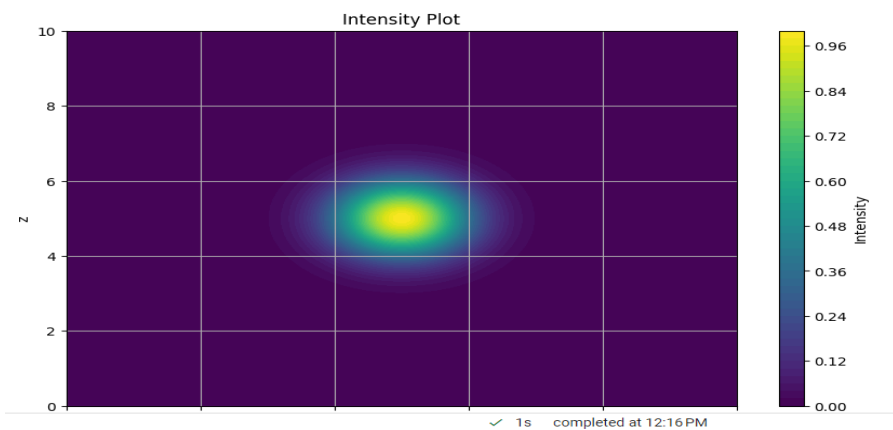
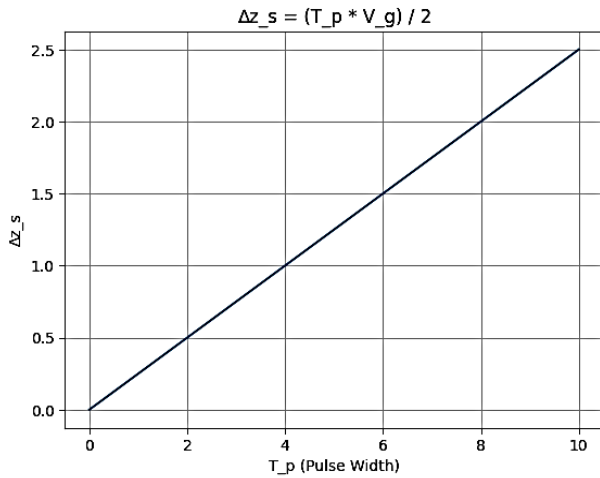


Figure 5.2: Intensity of the Backscattered Signal Spatial resolution of phase OTDR

In optical time-domain reflectometry (OTDR), the spatial resolution pertains to the system's capability to differentiate between two closely spaced events (reflections or backscatter) along the length of the fiber. This establishes the minimum separation between the two events that the Optical Time-Domain Reflectometer (OTDR) can distinguish. The spatial resolution is influenced by the pulse width of the probing signal used in the OTDR measurements. The spatial resolution, denoted as  $\Delta z_s$ , is given by formula:

$$\Delta z_s = \frac{T_p V_g}{2} \quad \text{----- (5.3)}$$



**Figure 5.3: Spatial resolution of the signal**

**Sensing range and repetition rate of a phase – OTDR**

**Sensing Range:** The sensing range of a phase-OTDR system refers to the distance over which the system can detect and analyze changes in fiber properties. They can vary from relatively short distances (hundreds of meters) to considerably long distances (over 100 km). The total sensing range depends on the Signal-to-Noise Ratio (SNR) of the system.

**SNR and the factors affecting it:** The SNR in a phase-OTDR system is a crucial factor that determines the ability of the system to distinguish between a weak backscattered signal and noise. This is influenced by various factors, including the following [13].

**Pulse Energy:** The energy of the probing pulse affects the amount of backscattered signal that is detected. A higher pulse energy can improve the SNR; however, there are practical limitations owing to nonlinear effects such as self-phase modulation.

**Fiber Attenuation Coefficient:** The Attenuation of the fiber causes the backscattered signal to weaken as it travels along the fiber. A lower attenuation results in a stronger backscattered signal and a better SNR.

**Wavelength:** The wavelength of the probing signal can also affect the SNR, and certain wavelengths are suitable for specific applications.

**Fiber Attenuation Coefficient:** The Attenuation of the fiber causes the backscattered signal to weaken as it travels along the fiber. A lower attenuation results in a stronger backscattered signal and a better SNR.

**Wavelength:** The wavelength of the probing signal can also affect the SNR, and certain wavelengths are suitable for specific applications.

**Detection Method and Sensing Range:** The detection method used in the phase-OTDR system affects the maximum sensing range. Coherent detection methods offer a higher SNR compared to direct detection but require a light source with higher coherence properties. The coherence length of the light source must exceed twice the maximum sensing distance to ensure correct demodulation of the backscattered signal.

**Repetition Rate and Impact on Detection:** The maximum repetition rate, denoted as  $T_R$ , is determined by the round-trip travel time of the probe pulse, fiber length (L), and group velocity ( $v_g$ ) of light in the fiber. This is represented by the following equation:

$$T_R = \frac{2L + w_p}{v_g} \quad \text{----- (5.4)}$$

Repetition rates, such as vibrations, are crucial for detecting periodic events in fibers. The acquisition frequency of traces dictates the upper limit of the detectable external event frequencies.

Simulating the backscattered light resulting from the propagation of a pulse through a SMF, the primary objective of the simulator is to mimic the laser pulse's journey within the examined fiber and calculate the backscattered field

detected by a coherent receiver (OTDR). This method, known as rapid time acquisition, involves gathering the intensity of backscattered light throughout the fiber length. To enhance the feasibility of the simulation and ease of computation, several simplifications are introduced into the model.

**Neglecting polarization effects:** This model does not consider the impact of polarization fading, which can occur in coherent-phase OTDR systems. This simplification helps reduce the complexity of the simulation.

**Ignoring the pulse-shape effects:** The model accepts a rectangular pulse shape and disregards the effects of different pulse shapes on the system. The utilization of a rectangular pulse shape is widespread, owing to its simplicity in manufacturing.

**Assuming ideal electronics:** The model assumes that electronic components, such as the analog-to-digital converter (ADC), work perfectly without any noise or non-ideal characteristics.

By incorporating these simplifications, the simulation becomes more manageable, although it may not accurately capture all the real-world effects.

During the simulation, two distinct factors—laser segment noise and laser flow—were considered to obtain more accurate results.

**Calculation of the Detected Intensity**

The computation of the detected intensity requires the determination of the number of scatterers, denoted as N, within the probing pulse at a specific time instant t.

$$\sum_{n=i}^{i+N} a[n] \exp(-2\alpha_A z[n]) \cos(2\pi\Delta v[n]t - 2\pi v[n]\tau_n + \vartheta_n[n])$$

$$\Delta v[n] = \Delta v_{fs} + \Delta v_d[n]$$

$$v[n] = v_o + \Delta v_d[n]$$

The laser phase term in Equation  $\vartheta_n[n]$  represents phase noise. Process for calculating the intensity term in the simulation [14]. The intensity was then demodulated back to the baseband using I/Q demodulation once in the baseband and the intensity was filtered using an (LPF) in the simulation.

A low-pass filter (LPF) was configured with a bandwidth exceeding 40% of the probe pulse bandwidth. This bandwidth adjustment is considered optimal for phase-OTDR systems employing rectangular probe pulses. By filtering the intensity with this LPF, the simulation aims to achieve the desired signal processing and optimize system performance.

**Phase Extraction and Unwarping**

When the In-phase and Quadrature phase signals were filtered to extract relevant information, the phase of the signal was computed. This phase computation involves determining the phase angle of the complex signal formed by combining In-phase and Quadrature phase components.

Mathematically, the phase  $\phi(t)$  of the complex signal is given by

$$\phi(t) = a \tan 2 \left( \frac{t(t)}{Q(t)} \right) \text{-----} (5.5)$$

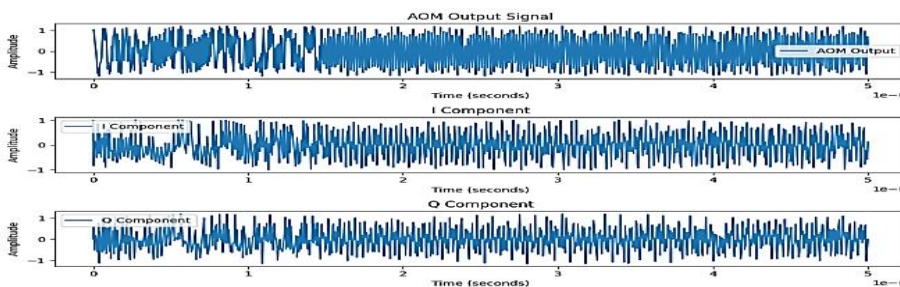


Figure 5.4: signal output waveform I and Q representation

The main issue is associated with the particular technique. This problem arises when noise is present in in-phase (I) and quadrature phase (Q) measurements, which can lead to errors in the phase-unwrapping algorithm. Specifically, if the true range is close to, then the algorithm may incorrectly assign a phase of  $\pm 2\pi$ . This erroneous assignment can result in significant differences in the development of the phase terms over time during fast acquisition.

### Phase unwrapping error:

In this example, we demonstrate a scenario in which a phase-unwrapping error occurs owing to the presence of phase noise. This situation involved the analysis of two consecutively acquired backscatter traces from a simulation.

In the figure, the initial trace illustrates the phase values between two data points with a difference smaller than  $\pi$ , whereas the 2nd trace demonstrates a phase difference exceeding  $\pi$ . This difference in the phase between these two traces is a direct result of the phase noise present in the simulation.

The top figure shows the resulting traces when a phase-unwrapping procedure was applied to the data. Here, a phase difference of approximately  $2\pi$  is introduced because of the unwrapping process. This demonstrates how phase noise and the unwrapping algorithm can lead to substantial variations in phase measurements between consecutive traces.

In summary, phase unwrapping errors can arise when the phase differences between consecutive data points are affected by phase noise. This can introduce significant variations in the measured phase values, leading to challenges in accurately interpreting phase information in certain scenarios.

The detection of alterations in the measured phase of a light pulse is limited to the duration during which the light pulse traverses a perturbed segment of the fiber [15]. The time at which the perturbed section was illuminated determined the total duration during which the phase changes could be observed and measured.

The time interval during which the perturbed section is subjected to the incident light from the laser pulse used in the phase-OTDR system,

$$T_L = \frac{(L+w_p)}{v_g} \text{ ----- (5.6)}$$

From equation (5.6) we write

$$\Delta\phi \propto \frac{2\pi}{\lambda} n\epsilon L \text{ ----- (5.7)}$$

Presuming that the fiber experiences sinusoidal strain at a frequency  $f$ ,

$$\Delta\phi = \frac{2\pi}{\lambda} n\epsilon L \sin(2\pi f T_L) \text{ ----- (5.8)}$$

### Backscatter Trace Phase Differential Analysis

Laser phase noise can significantly affect the performance of optical systems with long fibers. To address this issue, the phase-differential method is commonly employed as a mitigation technique. This method leverages the Gaussian white noise nature of laser phase noise and effectively reduces its influence through averaging [16].

The phase-differential method works by averaging multiple backscatter traces. At each spatial location along the fiber, the system acquires a certain number of traces (N) and averages them. Thus, the random fluctuations caused by the laser phase noise were smoothed out, leading to a reduction in noise and an improvement in the accuracy of the phase measurements.

However, tradeoffs are associated with this approach. As the system averaged over N traces at each spatial location, the effective slow-time acquisition rate decreased. This implies that more time is required to gather the required number of traces for each location, potentially affecting the ability of the system to capture time-varying phenomena rapidly along the fiber.

Furthermore, the extreme measurable frequency of the system is affected by the averaging process. By averaging multiple traces, the sensitivity of the system to high-frequency events is reduced, limiting its ability to detect rapid changes in the fiber properties.

Despite these trade-offs, the phase differential method offers valuable benefits. It effectively mitigates the laser phase noise by averaging, while maintaining the system's capability to detect events with higher frequencies. However, the application of this method results in a trade-off in terms of the compact spatial resolution. To utilize the phase

differential method, the fiber segment between points A and B was partitioned into smaller subsections with a length increment of  $\Delta z$ . Within each subsection, the system averages the phase values from multiple acquired traces, resulting in a more reliable representation of the phase behavior along the fiber.

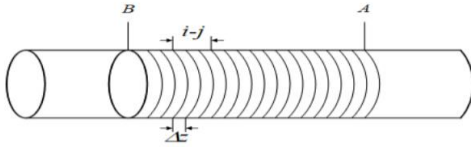


**Figure 5.5: Segmentation of sections within optical fibers**

Differential Averaging involves calculating the phase disparity between two spatial points, denoted as A and B, along the optical fiber. The phase difference  $\theta_{A,B}(t)$ , at time t was determined using Equation (5.9).

$$\theta_{A,B}(t) = \sum_{i=1+(A+B)/2}^A \sum_{j=B}^{i-1-(A-B)/2} \frac{(\theta_i(t) - \theta_j(t))(A-B)}{(i-j)N} \text{ ----- (5.9)}$$

The effectiveness of the Differential Averaging method in reducing noise is influenced by the decision regarding the sub-separation distances denoted as "i" and "j" significantly influences the overall outcome. Slighter partings between i and j generally result in higher accuracy, because averaging involves nearby data points. However, smaller separations also lead to more overlap between the computed subsections where averaging occurs. This overlap reduces the effectiveness of noise suppression because it introduces partial dependence between the computed subsections, thereby affecting the noise reduction capability of the method.

The figure 5.6 demonstrates how the choice of i and j affects the accuracy and noise reduction capabilities of the Differential Averaging method. Properly selecting the sub-separation distances is essential to strike a balance between accuracy and noise reduction in the phase measurements. Larger separations provide more independence between sub-sections but may sacrifice some accuracy, whereas smaller separations offer higher accuracy but may suffer from overlapping and reduced noise suppression effectiveness.

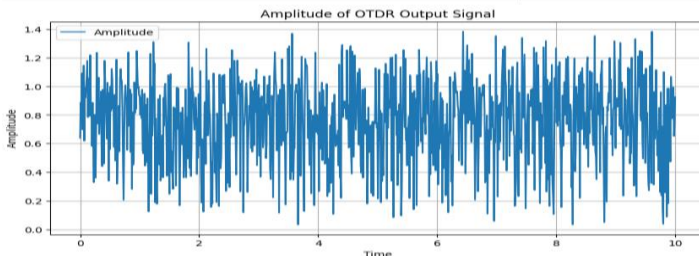


**Figure 5.6: Amplitude of the output waveform**

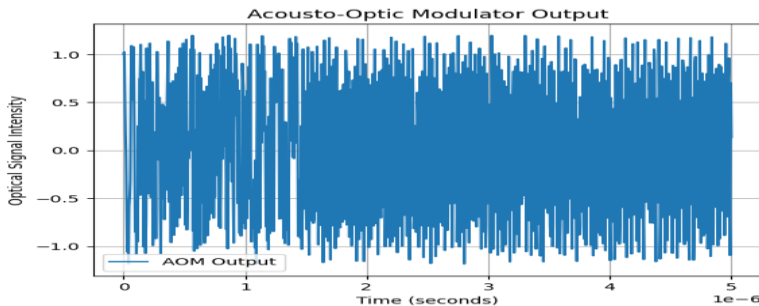


**Figure 5.7: Phase of the output waveform**

**Conclusion:** In this study, a statistical model for distributed acoustic sensor (DAS) interrogation units that employs fiber-optic cables and laser pulses for acoustic signal detection is proposed and examined. The model focuses on understanding the characteristics of backscattered signals generated in a fiber-optic cable under static conditions, where no external acoustic disturbances are present.

The key components of the model were the coherent components of the backscattered signals, namely, the amplitude and phase. Explicit equations were used to mathematically represent these components, providing a foundation for understanding the behavior of fiber-optic cables and their interactions with the laser pulses.

The amplitude component of the backscattered signal represents the strength of the signal, whereas the phase component indicates timing. By analyzing these components, we were able to make predictions regarding the signal spectrum and autocorrelation characteristics.

The experimental validation was performed using Python coding, and the model predictions were found to be in good agreement with the experimental findings. This confirms the accuracy and efficacy of the proposed model for DAS signal interrogation.

This study explored various components essential for Distributed Acoustic Sensing (DAS) systems. This includes an in-depth discussion of the coherent narrowband laser source, acoustic–optic modulator, Erbium-Doped Fiber Amplifier (EDFA), and dynamics of light propagation in a single-mode fiber. Additionally, a thorough examination of the phase-based optical time-domain reflectometry (OTDR) system was conducted with a particular focus on its applications in sensing.

Overall, this study contributes significantly to the advancement of the DAS technology. The developed statistical model allows for a better understanding of the behavior of fiber-optic cables under static conditions and provides valuable insights for optimizing and improving DAS systems. As Distributed Acoustic Sensing (DAS) continues to find applications in diverse fields such as structural health monitoring, security, and geophysical exploration, the findings of this model will be instrumental in enhancing the overall efficiency and accuracy of DAS-based sensing systems.

## ACKNOWLEDGEMENTS

We would like to express our sincere gratitude to Dr. A. Robert Sam, Scientist in Charge at CSIR-CSIO, and Dr. G.S. Ayyappan, Senior Principal Scientist at CSIR-CSIO, for their invaluable guidance and support throughout this project. The authors declare that there are no conflicts of interest regarding the publication of this manuscript.

## REFERENCES

- [1]. Tiange Wu, Guowei Liu, Shenggui Fu \* and Fei Xing, “Recent Progress of Fiber-Optic Sensors for the Structural Health Monitoring of Civil Infrastructure,” Received: 27 June 2020; Accepted: 10 August 2020; Published: 12 August 2020
- [2]. DONG XinTong, LI Yue, LIU Fei, FENG QianKun, ZHONG Tie. The new suppression technology for random noise in DAS seismic data is based on a convolutional neural network. 2021
- [3]. Hugo F. Martins, Sonia Mart´ın-L´opez, Pedro Corredera, Massimo L. Filograno, Orlando Fraz˜ao, and Miguel Gonzalez-Herr´aez, *Senior Member, OSA* “Phase-sensitive Optical Time Domain Reflectometer Assisted by First-order Raman Amplification for Distributed Vibration Sensing Over >100 km” JOURNAL OF LIGHTWAVE TECHNOLOGY, VOL. 32, NO. 8, APRIL 15, 2014
- [4]. Yonas Muanenda “Recent Advances in Distributed Acoustic Sensing Based on Phase-Sensitive Optical Time Domain Reflectometry” Received 13 October 2017; Revised 28 March 2018; Accepted 5 April 2018; Published 13 May 2018
- [5]. Peter G. Hubbard, James Xu, Shenghan Zhang, Matthew Dejong, Linqing Luo, Kenichi Soga, Carlo Papa, Christian Zulberti, Demetrio Malara, Fabio Fugazzotto, Francisco Garcia Lopez & Chris Minto. Dynamic structural health monitoring of model wind turbine tower using distributed acoustic sensing (DAS). Pages 833–849 (2021).
- [6]. K. Takada; H. Yamada: Narrowband light source with an acoustooptic tunable filter for optical low-coherence reflectometry.

- [7]. : Shang, Y.; Sun, M.; Wang, C.; Yang, J.; Du, Y.; Yi, J.; Zhao, W.; Wang, Y.; Zhao, Y.; Ni, J. Research Progress in Distributed Acoustic Sensing Techniques. *Sensors* 2022, 22, 6060. <https://doi.org/10.3390/s22166060>.
- [8]. Zejie Yu and Xiankai Sun; Acousto-optic modulation of photonic bound state in the continuum; *Science & Applications* (2020) 9:1
- [9]. Mahmoud M. A. Eid and Ahmed Nabih Zaki Rashed; Simulative and analytical methods of bidirectional EDFA amplifiers in optical communication links in the optimum case;
- [10]. M. E. FERMAN, S. B. POOLE, D. N. PAYNE, AND F. MARTINEZ; Comparative Measurement of Rayleigh scattering in Single-Mode Optical Fibers Based on an OTDR Technique
- [11]. Xiaoyi Bao and Yuan Wang; Recent Advancements in Rayleigh Scattering-Based Distributed Fiber Sensors; Published 11 March 2021.
- [12]. Pedro Tovar, Bismarck Costa Lima, and Jean Pierre von der Weid; Modelling Intensity Fluctuations of Rayleigh Backscattered Coherent Light in Single-Mode Fibers; Modelling Intensity Fluctuations of Rayleigh Backscattered Coherent Light in Single-Mode Fibers.
- [13]. Massimo Leonardo Filograno, Christos Riziotis \*and Maria Kandyla; a Low-Cost Phase-OTDR System for Structural Health Monitoring: Design and Instrumentation
- [14]. Michael Brown; Simulation of Coherent Phase Optical Time-Domain Reflectometry; Copyright©2017.
- [15]. Y. Shi, H. Feng, and Z. Zeng, "A long distance phase-sensitive optical time domain reflectometer With a simple structure and high locating accuracy," *Sensors (Switzerland)*, vol. 15, no. 9, pp. 21957–21970, 2015.
- [16]. Y. Koyamada, M. Imahama, K. Kubota, and K. Hogari, "Fiber-optic distributed strain and temperature sensing with very high measurand resolution over long range using coherent OTDR," *J. Lightw. Technol.*, vol. 27, no. 9, pp. 1142–1146, May 2009